Progress In Electromagnetics Research B, Vol. 5, 303–321, 2008

UPLINK CARRIER-TO-INTERFERENCE IMPROVEMENT IN A CELLULAR TELECOMMUNICATION SYSTEM WHEN A SIX-BEAM SWITCHED PARASITIC ARRAY IS IMPLEMENTED

A. I. Sotiriou, P. T. Trakadas, and C. N. Capsalis

Division of Information Transmission Systems and Material Technology
Department of Electrical and Computer Engineering
National Technical University of Athens
9, Iroon Polytechniou Str., 15773 Athens, Greece

Abstract—Mobile broadband communication is experiencing rapid growth in the following sections: technology, range of services and marketing target groups. This growth has driven research and development activities towards advanced high-data-rate wireless systems, with improved network performance. A typical example of technology thrust in wireless communications is the use of adaptive antennas at the transceivers, in association with advanced array signal processing. Although the mass deployment of adaptive array systems has not achieved the desired levels yet, there are many examples of improved cell coverage, link quality and system capacity at several networks. The performance of a six-beam switched parasitic array, in terms of carrier-to-interference ratio (CIR) measurement at the uplink direction, is presented in this paper. The switched parasitic array is designed with the aid of the method of genetic algorithms and the simulation results are compared with respect to those obtained when an omni directional antenna is used instead. The calculated CIR improvement reveals the superiority of the adaptive system compared to the conventional one.

1. INTRODUCTION

The implementation of smart antenna techniques, in existing as well as future wireless systems, is expected to have a strong impact on efficient spectrum use, cost minimization for establishing new wireless networks and service quality enhancement. Nevertheless, the successful

adoption of adaptive systems relies on taking into consideration the particular technology features at an early stage. Network operators are obliged to optimize the trade-off between complexity and performance and respond to the critical question: in which occasions a smart antenna system has to be deployed? In the mean time, they have to consider several issues, such as re-configurability to varying channel propagation, multi-user diversity, as well as the design of a suitable simulation methodology and the accurate modeling of channel characteristics, interference and implementation losses [1].

A more efficient and flexible network infrastructure could be built with the help of smart antennas on condition that sufficient amount of data traffic is generated by the users. Factors that will increase overall traffic are mobile penetration and traffic density per-user, which are both triggered by new enhanced services. Therefore, sufficient network capacity must be available through higher capacity gain. However, this extra capacity is more likely to be necessary only in highly dense urban environments, but even more in technical parks and business centers, where numerous business users have their work place [2].

Several novel methods have been proposed for beamforming, null steering and direction-of-arrival finding [6–12], for almost all antenna types. Even more, there is a constant and intensive development of adaptive antenna models [13–15]. In addition to the aforementioned benefits, extended range and gap filling can be dealt with, when an adaptive antenna is implemented at the base station. The gain towards user of interest is increased, resulting in a longer reception range. Furthermore, adaptive antennas are able to reduce or even mitigate the impact of imperfect power control, since the uplink signals from different users are better-isolated (near-far problem). The power radiated from conventional base station antennas, irrespective of the user of interest location, acts as interference to all other users within the same area. The result is the degradation of system performance; namely CIR and Bit-Error-Rate (BER) are decreasing. Moreover, the introduction of adaptive antennas in the communication system enables users and base station to operate with much lower transmitted power, reducing interference levels to all other users within the same area. In this way, both CIR and BER are improved and frequency reuse can be tighter, providing extra capacity to the system [3–5].

Switched parasitic arrays, both with linear and planar configuration of their antenna elements, can be implemented for electronic beam steering. An appropriate N-length (where N denotes the number of antenna elements) digital codeword, consisting of 1 s and 0 s, is applied to the antenna feeding circuit. Each digital codeword determines a unique radiation pattern among $2^N - 1$ possible ones. The 1 s and 0 s

represent the active and parasitic elements of the array, respectively. Linear arrays have a symmetrical radiation pattern in the azimuth plane. On the contrary, planar arrays cover the whole azimuth plane and therefore offer main beams every $(360/q)^\circ$, where q denotes the number of different main beams [16].

In this paper, the performance of a seven-element switched parasitic planar array is evaluated in terms of CIR improvement, when the antenna system is installed at a Base Transceiver Station (BTS), instead of an omni directional antenna. Several simulations have been performed for four different types of base stations: macro BTS, midi BTS, micro BTS and pico BTS. In all simulations, both power control and no power control cases have been taken into consideration. The next section analyzes the benefits derived from smart antenna deployment; Section 3 presents the antenna design method and rules, while in Section 4 the simulation model is described. Section 5 presents simulation results and finally Section 6 summarizes the conclusions.

2. MOST SIGNIFICANT BENEFITS FROM SMART ANTENNA DEPLOYMENT

In the following paragraphs, the most significant benefits from smart antenna deployment are shortly presented.

2.1. Increased Transmission Data Rates

Traditional cellular systems are constantly trying to meet the requirements of new demanding services. It is true that in some densely populated business areas, high-data-rates are required, which cannot be achieved with a conventional antenna system. As described in [17], increased processing across the spatial domain seems to be the only means for fulfilling the above needs and providing the customers with the appropriate transmission data-rates. Even more, in [3] and [18] it is clearly stated that the combined use of M-element transmit and receive arrays offer M-fold improvement in data-rate transmission.

2.2. Increased Coverage Range

In rural areas, not densely populated, radio coverage is far more important than capacity. As adaptive antennas are more directional than traditional sector or omni directional antennas, the coverage area offered to subscribers is enlarged [19]. The increased antenna gain in dB of a multi-element antenna, compared to the gain of a single-element antenna, is roughly equal to the total number of antenna

elements, e.g., a seven-element array can provide an extra gain of 7 dB [3]. In this way BTSs can be installed further apart, leading to a more cost-efficient deployment. As shown in [18], a ten-element antenna is capable of doubling the coverage area of a BTS.

2.3. Capacity Increase

The performance of Time Division Multiple Access (TDMA) systems is directly dependent on interfering signals. The presence of undesired radiation, especially in densely populated areas, is the main noise source for mobile communications, rendering those systems interference limited. The CIR affects BER to a larger extent than Signal-to-thermal Noise Ratio (SNR) and therefore needs to be carefully monitored and evaluated. Adaptive antenna systems suppress the interfering signals by minimizing the gain towards their direction, whereas the gain towards the signal of interest is maximized. In [3], it is stated that experimental results have reported up to 10 dB increase in average CIR in urban areas. In TDMA systems, improved CIR allows for tighter frequency reuse and reduced cell clusters. Simulation results have shown that a four-element adaptive array permits frequency reuse at every cell in a three-sector system, for a sevenfold capacity increase [18].

3. DESIGN OF A SWITCHED PARASITIC ARRAY USING A GENETIC ALGORITHM

In the following paragraphs the basic design guidelines for the proposed switched parasitic array are analyzed.

3.1. Switched Parasitic Planar Arrays

The mathematical model for the array factor $AF(\theta, \phi)$ of an N-dipole planar array lying in the azimuth plane (N dipoles parallel to the z-axis, with their centers in the horizontal plane) is given by [16]

$$AF(\theta, \phi) = \sum_{m=1}^{N} c_m e^{jkr_m \sin\theta \cos(\phi - \phi_m)} \tag{1}$$

where:

$c_m = \frac{I_m}{I_1}$ the relative excitation coefficients, I_m stands for the excitation base current of the m-th element and I_1 the excitation base current of element 1.

$k = \frac{2\pi}{\lambda}$, λ being the wavelength.

$r_m = \sqrt{x_m^2 + y_m^2}$, (x_m, y_m) the azimuth coordinates of element m.

$\phi_m = \arg(x_m + jy_m)$, the azimuth angle of element m and θ the elevation angle, being equal to 90° for the remainder of this paper.

The radiation pattern in the azimuth plane of a planar array, whose elements are considered as dipoles of length L, is given by

$$U(\theta = 90^\circ, \phi) = \mathrm{A} \cdot |AF(\theta = 90^\circ, \phi)|^2 \tag{2}$$

where A is a constant value depending on the radiation pattern of a single element $U_o(\theta = 90^\circ, \phi)$. The elements excitations I_m $(m = 1 \ldots N)$ are related to the input voltages V_m, with equal amplitudes but different phase values, by the impedance matrix $\mathbf{Z}$:

$$\mathbf{V} = \mathbf{Z} \cdot \mathbf{I} \tag{3}$$

where $\mathbf{V}$ and $\mathbf{I}$ are the voltage and current vectors, respectively

$$\mathbf{V} = [V_1 \quad \ldots \quad V_N]^T \tag{4}$$

$$\mathbf{I} = [I_1 \quad \ldots \quad I_N]^T \tag{5}$$

$$\mathbf{Z} = \begin{bmatrix} Z_{11} & Z_{12} & \ldots & Z_{1N} \\ Z_{21} & Z_{22} & \ldots & Z_{2N} \\ \cdot & \cdot & & \cdot \\ \cdot & \cdot & & \cdot \\ Z_{N1} & Z_{N2} & \ldots & Z_{NN} \end{bmatrix} \tag{6}$$

Through (3)–(6), the terminal voltage of any one element can be expressed in terms of the currents flowing in the others, mutual impedance and self impedance:

$$V_n = \sum_{m=1}^{N} Z_{nm} I_m \qquad n = 1 \ldots N \tag{7}$$

where

Z_{nm} the mutual impedance between elements n, m.

Z_{mm} the self impedance of element m.

The self impedance (referred to at the input base current I_i) of a dipole of length L, is given by [16]

$$Z_i = -\frac{1}{I_i^2} \int_{-L/2}^{L/2} E_z(\rho = a, z)\, I(z)\, dz \tag{8}$$

where

$$I(z) = I_{\max} \sin\left[k\left(\frac{L}{2} - |z|\right)\right] \tag{9}$$

the current distribution

E_z the tangential electric field along the surface of the dipole and a the dipole radius.

The mutual impedance (referred to at the input base current I_{1i} of dipole 1), between two parallel dipoles at a distance d, is given by [16]

$$Z_{21i} = \frac{V_{21}}{I_{1i}} = -\frac{1}{I_{1i}I_{2i}} \int_{-L_2/2}^{L_2/2} E_{z21}(z)\, I_2(z)\, dz \tag{10}$$

where

V_{21} the voltage induced in dipole 2 because of the current flowing in dipole 1.

E_{z21} E-field component along the surface of dipole 2 radiated by dipole 1, which is parallel to dipole 2.

I_2 current distribution along dipole 2.

Equations (8) and (10) can be solved and give the self and mutual impedance as functions of the ratios $\frac{L}{\lambda}$, $\frac{a}{\lambda}$ and $\frac{L_1}{\lambda}$, $\frac{L_2}{\lambda}$, $\frac{d}{\lambda}$, respectively [16]. As far as the input impedance to each active element of the array is concerned, well-known impedance matching techniques may be deployed [16].

3.2. Antenna Design with Genetic Algorithm

The use of genetic algorithms for antenna design purposes and electronic beam steering is a well-known method introduced in the last decade [20–25]. For the design of the antenna used in this paper, roulette wheel selection, simple crossover with $p_{crossover} = 0.8$ and binary mutation with $p_{mutation} = 0.04$ were employed. The objective was to cover the entire azimuth plane with main beams every 60°, having relative side lobe levels lower than -3 dB [26]. The design was made feasible by selecting the appropriate digital code words, among the $2^N - 1$ available, which maximize the objective function containing the pattern requirements. Each digital codeword implies which of the antenna elements are fed with voltage (active) and which are short-circuited (parasitic). Tables 1 and 2 provide the

directional and geometrical characteristics of the designed 7-dipole array, respectively [26].

An RF switch is connected to each antenna element. A phase shifter is also connected to each element, after the RF switch,

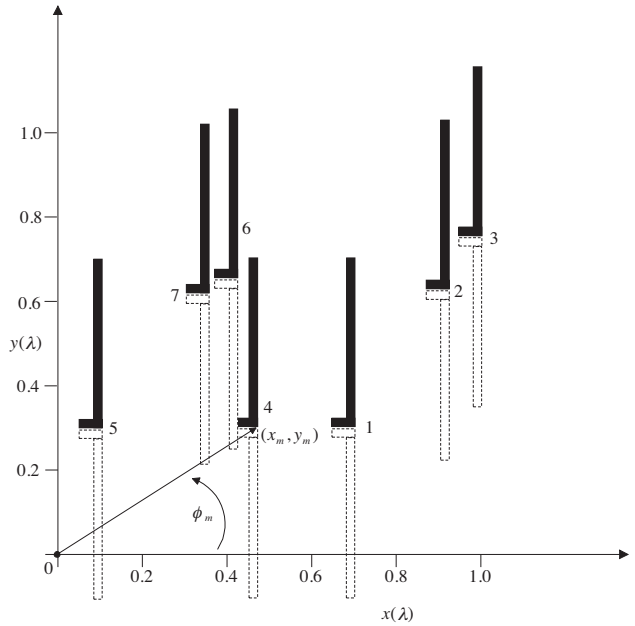

Figure 1. Geometry of the six-beam switched parasitic array [26].

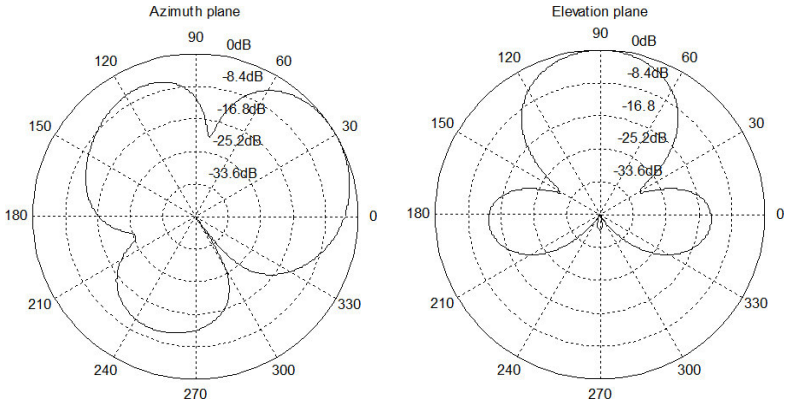

Figure 2a. Normalized radiation patterns ($\varphi_{\max} = 31.1°$, $\theta_{\max} = 90°$) of the 7-dipole array [26].

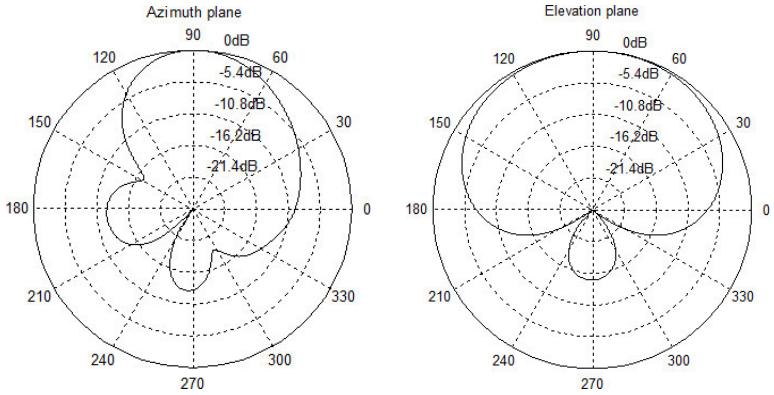

Figure 2b. Normalized radiation patterns ($\varphi_{\max} = 89.2°$, $\theta_{\max} = 90°$) of the 7-dipole array [26].

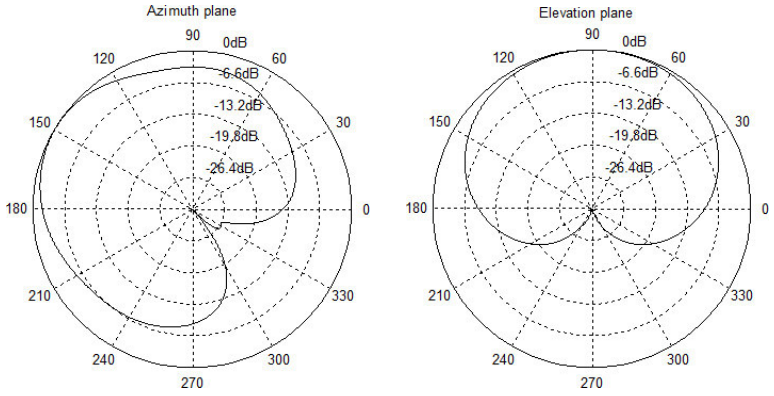

Figure 2c. Normalized radiation patterns ($\varphi_{\max} = 148.1°$, $\theta_{\max} = 90°$) of the 7-dipole array [26].

determining the appropriate voltage phase value δ_m for each feed configuration. When the RF switch is "on", the input voltage is equal to $V_m = A\exp(j\delta_m)$, otherwise the RF switch is "off" and a short circuit is applied to the antenna element.

Each array dipole has length $L = \lambda/2$, radius $\alpha = 0.001\lambda$ and its axis parallel to the z-axis, while its feeding point lies in the x-y plane. Simulations at different frequencies prove that the array described in Tables 1 and 2 is a narrowband one and its bandwidth is 2.5% of the carrier frequency [26]. Figure 1 presents the array configuration in the azimuth plane and Figures 2(a) to 2(f) depict the six possible

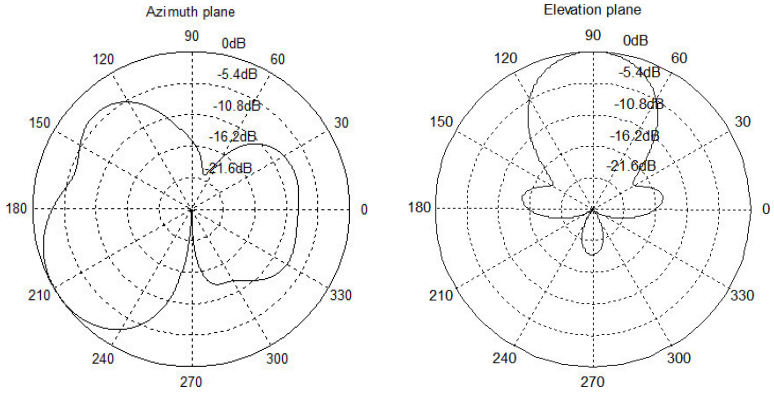

Figure 2d. Normalized radiation patterns ($\varphi_{\max} = 211.9°$, $\theta_{\max} = 90°$) of the 7-dipole array [26].

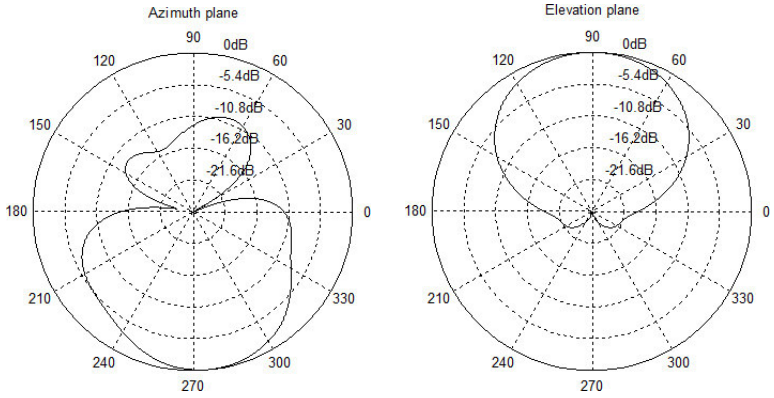

Figure 2e. Normalized radiation patterns ($\varphi_{\max} = 276.4°$, $\theta_{\max} = 90°$) of the 7-dipole array [26].

radiation patterns of the considered array in both the azimuth and elevation plane.

4. SIMULATION MODEL DESCRIPTION

Interference issues are and will remain the most important factors in telecommunication system performance degradation. The beamforming technique is widely used in cellular mobile communication systems, in order to optimize the usage of frequency resources [4, 27]. Implementing this technique at the base station, co-channel interference and

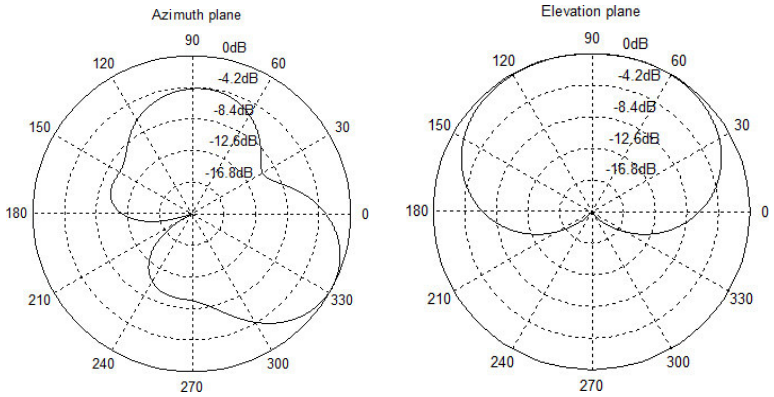

Figure 2f. Normalized radiation patterns ($\varphi_{\max} = 332.4°$, $\theta_{\max} = 90°$) of the 7-dipole array [26].

reception of excess multipath fading from undesired directions can be significantly reduced. As a result, the service quality at both base and mobile station is improved. The ratio of the desired signal to the total of received co-channel interference, CIR, is the key parameter that determines the capacity of the telecommunication system. With beamforming, CIR can be optimized and therefore improve system capacity.

The objective of this paper is to demonstrate the main advantages related to the use of the 7-dipole switched beam antenna array at the base station, instead of an omni directional antenna. There are several measures to evaluate the effect of beamforming, mainly depending on the access scheme. In the present paper, the CIR parameter has been chosen, as it is common in all access schemes. At this stage, simulation results are focused only on the uplink direction. A network of nineteen base stations, equipped with the switched beam antenna array, has been considered with cluster size equal to three. The radius of the base station covering area has been selected equal to 30 m for the picocell case, 100 m for the microcell case, 500 m for the midicell case and 1–3 Km for the macrocell case. The height of the base stations is summarized in the following table for each case.

In all the above cases, both power control and no power control conditions have been applied to the mobile station transmitter. The latter has been considered to be equipped with an omni directional antenna. In the no power control condition, the mobile station transmitted power is equal to the propagation loss from the cell boundary to the base station. In the power control condition, the mobile station transmits with power equal to its current propagation loss enhanced by a power margin. In this paper, the power margin has

Table 1. Directions of maximum gains, 3 dB beam widths, and relative side lobe levels for the 7-element array [26].

Digital codeword	**Maximum gain direction** $\phi_{\max}$ (°)	$\phi^{-}_{-3\,\mathrm{dB}}$ (°)	$\phi^{+}_{-3\,\mathrm{dB}}$ (°)	$\Delta\phi_{-3\,\mathrm{dB}}$ (°)	**Relative side lobe level S.L.L.(dB)**
0110010	31.10	2.03	55.84	53.81	−5.56
0000011	89.18	54.89	114.85	59.96	−12.41
0000001	148.12	109.00	189.49	80.49	−3.32
0101100	211.98	180.71	239.96	59.25	−3.73
1100000	276.42	240.33	310.88	70.55	−8.94
1010000	332.43	305.29	359.16	53.87	−4.14

Table 2. Element coordinates and constant phases for the 7-element array [26].

Element	$\mathbf{x_m(\lambda)}$	$\mathbf{y_m(\lambda)}$	$\boldsymbol{\delta_m}$**(rad)**
1	0.68269	0.29063	0.42339
2	0.87479	0.63954	2.61452
3	0.95015	0.74330	0.35733
4	0.43318	0.29939	4.74985
5	0.10149	0.31746	2.69084
6	0.39505	0.64619	4.41774
7	0.32344	0.60335	5.72366

Table 3. Calculated impedance matrix Z.

$$Z=\begin{bmatrix} 73.1+42.2i & 6.6-37.4i & -16.2-26.7i & 40.9-28.3i & -22.0-18.7i & -5.3-34.2i & -8.7-32.5i \\ 6.6-37.4i & 73.1+42.2i & 63.7-1.0i & -20.2-21.8i & -14.6+15.4i & -9.3-32.1i & -19.3-23.0i \\ -16.2-26.7i & 63.7-1.0i & 73.1+42.2i & -25.2-2.4i & -1.6+19.0i & -20.4-21.4i & -25.0-9.2i \\ 40.9-28.3i & -20.2-21.8i & -25.2-2.4i & 73.1+42.2i & 21.6-36.7i & 16.4-37.5i & 22.5-36.5i \\ -22.0-18.7i & -14.6+15.4i & -1.6+19.0i & 21.6-36.7i & 73.1+42.2i & -2.2-35.4i & 14.7-37.6i \\ -5.3-34.2i & -9.3-32.1i & -20.4-21.4i & 16.4-37.5i & -2.2-35.4i & 73.1+42.2i & 69.0+12.8i \\ -8.7-32.5i & -19.3-23.0i & -25.0-9.2i & 22.5-36.5i & 14.7-37.6i & 69.0+12.8i & 73.1+42.2i \end{bmatrix}$$

Table 4. Base station heights for each cell type.

	Picocell case	Microcell case	Midicell case	Microcell case
Base station height	5 m	10 m	20 m	0 m
	10 m	20 m	40 m	
	15 m	30 m	60 m	

been chosen equal to 3 dB. For all simulations, except for the macrocell case, the down tilt of the switched beam antenna array is varying from 0° to 30°.

In the initial stage of the simulation process, the positions of the base stations and mobile users are calculated. One mobile user per base station is considered and its position within the covering area is following a random distribution. In the second simulation step, distances, azimuth and elevation angles between the mobile users and the central base station under evaluation are calculated. In the next stage, the active radiation pattern at the base station under evaluation is determined. Finally, the received signal level from all mobile users at the central base station is calculated and therefore the CIR is determined.

A second set of simulations has also been performed, this time considering that the switched beam antenna array is used at both base station and mobile user devices. The main process remains the same, as previously described, with the exception that the active radiation pattern has to be determined not only for the central base station but also for all the mobile users.

5. SIMULATION RESULTS

The following Figures 3(a)–3(d) present simulation results, for all types of cells, in the scenario where the switched parasitic planar array (SPPA) is implemented only at the base station. It is clear that, for all base station types, there is a significant improvement in the CIR, ranging from 4 dB up to 13 dB. It is also obvious that, in the majority of the simulations, the results with the power control condition are superior to those without the condition. This is expected, as mobile users closer to the base stations transmit with lower power than without the power control condition, thus minimizing interference to all the other base stations. Another important notice is that down tilt is a significant factor in the interference mitigation issue, with

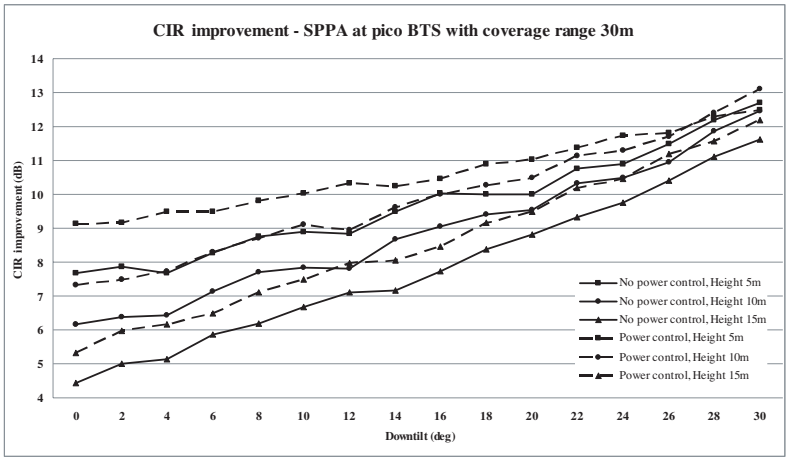

Figure 3a. CIR improvement with the SPPA at picocell base station.

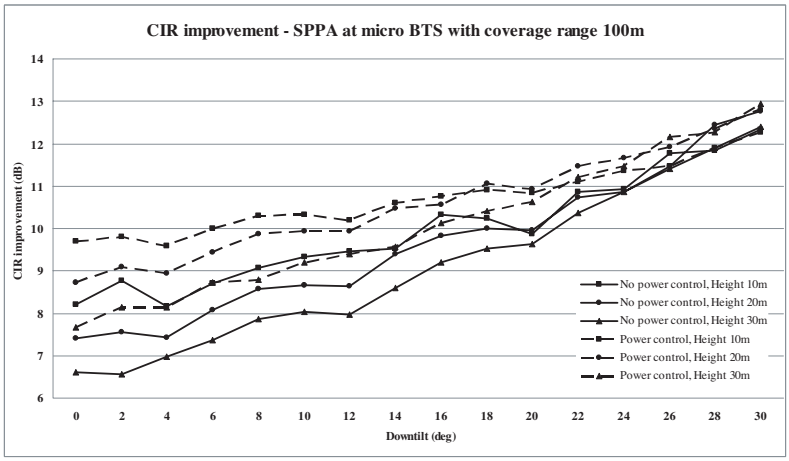

Figure 3b. CIR improvement with the SPPA at microcell base station.

higher down tilt values further improving the CIR. It is true that high down tilt values prevent the BTS antenna from receiving signals outside the designed cell boundary, especially when the elevation plane is considered. The antenna used in this paper is quite wide in the elevation plane. An antenna being less wide in this plane could result in an even better CIR improvement as the antenna reception would be further restrained within the designed coverage area, limiting

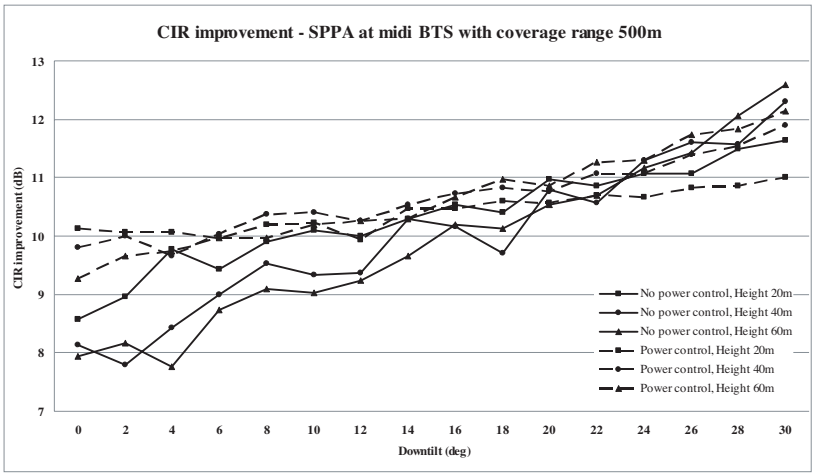

Figure 3c. CIR improvement with the SPPA at midicell base station.

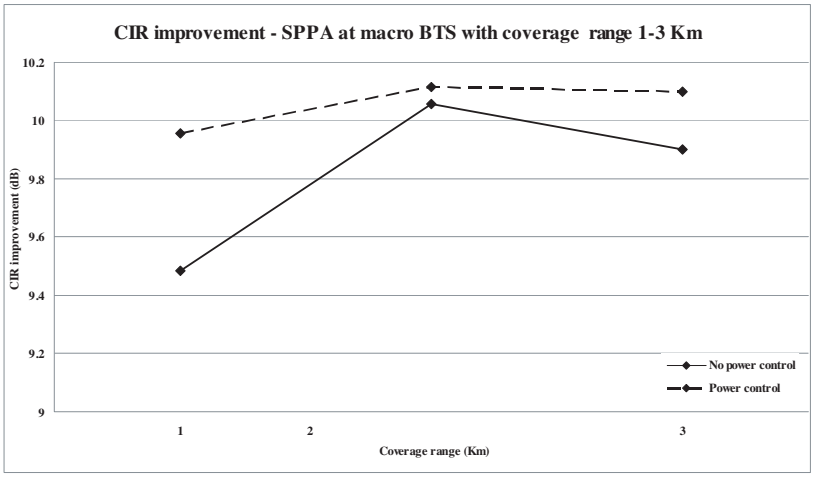

Figure 3d. CIR improvement with the SPPA at macrocell base station.

the receiving signals from users outside the BTS's area. Another notice that can be made is that increasing the antenna height, CIR improvement becomes less. With the antenna height increase, the cell's offered coverage is enlarged and therefore signals from users of no interest are received.

Figures 4(a)–4(d) depict simulation results with the SPPA deployed both at base station and mobile user devices. It is easily

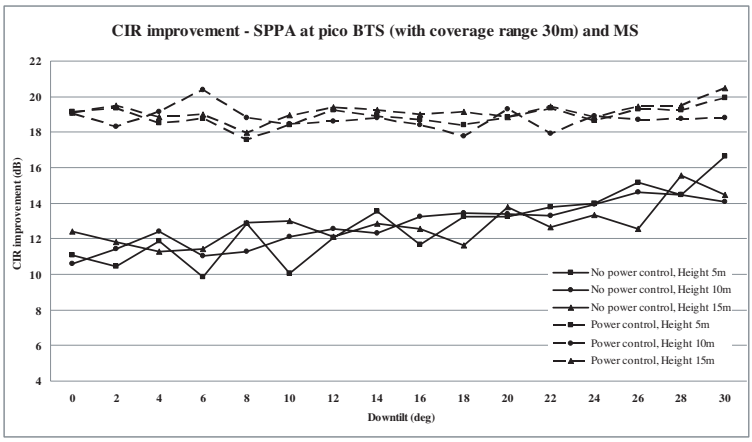

Figure 4a. CIR improvement with the SPPA both at picocell base station and mobile terminal.

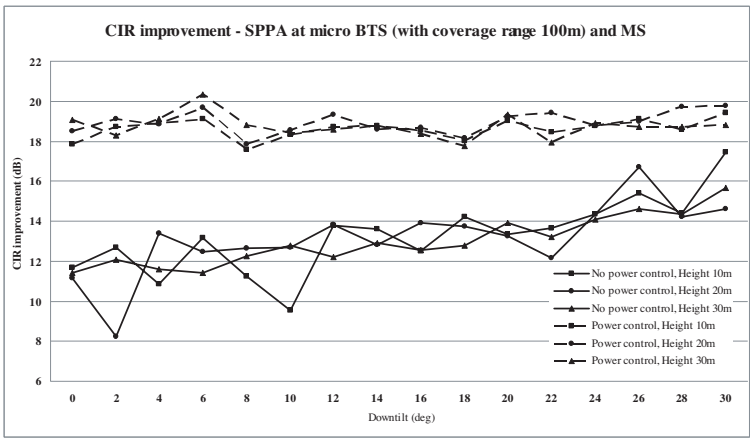

Figure 4b. CIR improvement with the SPPA both at microcell base station and mobile terminal.

noticeable that the implementation of beamforming at both ends of the communication channel provides a major quality improvement. In the picocell case without power control, an extra CIR improvement of approximately 6 dB is achieved. In the same case, but applying the power control condition, the extra CIR improvement varies from 7 dB–12 dB, providing the communication system with a composite CIR improvement of 18 dB–20 dB. Similar observations can be made for the remaining cell type cases.

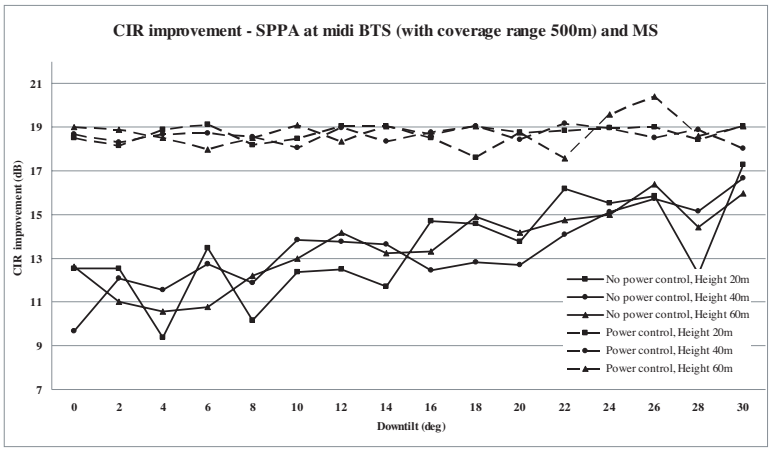

Figure 4c. CIR improvement with the SPPA both at midicell base station and mobile terminal.

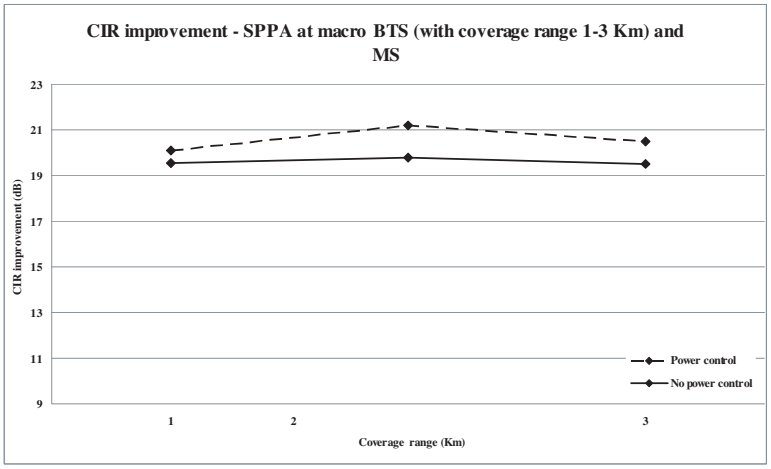

Figure 4d. CIR improvement with the SPPA both at macrocell base station and mobile terminal.

In this set of simulations, the power or no power control condition has a more considerable influence, providing an extra CIR gain of 5 dB–8 dB (compare Figures 4(a)–4(d) with Figures 3(a)–3(d). This is a reasonable fact, since the decrease in the transmitted power, due to power control, as well as the orientation of the mobile station antenna, due to beamforming, minimize the undesired radiation towards the central base station.

6. CONCLUSIONS

In this paper, a previously designed [26] seven-element switched parasitic planar array is proposed, in order to mitigate interference effects. In the first simulations set, the antenna has been considered only at the base stations of a cellular system equipped with nineteen base stations. The results show a significant CIR improvement of approximately 4 dB–13 dB, especially if power control condition is applied at the mobile terminals. In the second simulations set, the antenna has been considered both at base stations and mobile terminals. The results are even better in the latter case, showing an improvement of 18 dB–20 dB, when the power control feature is activated.

REFERENCES

1. Alexiou, A. and M. Haardt, "Smart antenna technologies for future wireless systems: Trends and challenges," *IEEE Communications Magazine*, Vol. 42, No. 9, 90–97, September 2004.
2. Glazunov, A., P. Karlsson, and R. Ljung, "Cost analysis of smart antenna systems deployment," *Vehicular Technology Conference, VTC 2005-Spring*, Vol. 1, No. 30, 329–333, 2005 IEEE 61st, June 2005.
3. Lehne, P. H. and M. Pettersen, "An overview of smart antenna technology for mobile communication systems," *IEEE Communications Surveys*, Vol. 2, No. 4, 2–13, Fourth Quarter, 1999.
4. Liberti, J. C. and T. S. Rappaport, *Smart Antennas for Wireless Communication: IS-95 and Third Generation CDMA Applications*, Prentice Hall, 1999.
5. Sotiriou, A. I., P. K. Varlamos, P. T. Trakadas, and C. Capsalis, "Performance of a six-beam switched parasitic planar array under one path Rayleigh fading environment," *Progress In Electromagnetics Research*, PIER 62, 89–106, 2006.
6. Gu, Y. J, Z. G. Shi, K. S. Chen, and Y. Li, "Robust adaptive beamforming for a class of Gaussian steering vector mismatch," *Progress In Electromagnetics Research*, PIER 81, 315–328, 2008.
7. Gu, Y. J., Z. G. Shi, K. S. Chen, and Y. Li, "Robust adaptive beamforming for steering vector uncertainties based on equivalent DOAs method," *Progress In Electromagnetics Research*, PIER 79, 277–290, 2008.

8. Varlamos, P. K., S. A. Mitilineos, S. C. Panagiotou, A. I. Sotiriou, and C. N. Capsalis, "Direction-of-arrival estimation approach using switched parasitic arrays," *Advances in Direction-of-Arrival Estimation*, Ch. 8, 145–160, Norwood, Artech House.
9. Mouhamadou, M., P. Vaudon, and M. Rammal, "Smart antenna array patterns synthesis: Null steering and multi-user beamforming by phase control," *Progress In Electromagnetics Research*, PIER 60, 95–106, 2006.
10. Jwa, H. and S. Bang, "Hybrid beamforming in WCDMA antenna array system," *Vehicular Technology Conference, 2004. VTC2004-Fall. 2004 IEEE 60th*, Vol. 1, 252–255, 2004.
11. Nishio, T., Y. Wang, and T. Itoh, "A high-speed adaptive antenna array with simultaneous multiple-beamforming capability," *Microwave Symposium Digest, 2003 IEEE MTT-S International*, Vol. 3, 1673–1676, 2003.
12. Ozdemir, O. and M. Torlak, "Opportunistic beamforming with partial channel state information," *Communications, 2006 IEEE International Conference on*, Vol. 12, 5313–5318, 2006.
13. Fakoukakis, F. E., S. G. Diamantis, A. P. Orfanides, and G. A. Kyriacou, "Development of an adaptive and switched beam smart antenna system for wireless communications," *Journal of Electromagnetic Waves and Applications*, Vol. 20, No. 3, 399–408, 2006.
14. Nakane, Y., T. Noguchi, and Y. Kuwahara, "Trial model of adaptive antenna equipped with switched loads on parasitic elements," *Antennas and Propagation, IEEE Transactions on*, Vol. 53, Issue 10, 3398–3402, 2005.
15. Kawitkar, P. and D. G. Wakde, "Design of digital prototype of adaptive antenna receiver," *Personal Wireless Communications, ICPWC 2005, 2005 IEEE International Conference on*, 334–338, 2005.
16. Balanis, C. A., *Antenna Theory Analysis and Design*, 3nd edition, John Wiley and Sons, 2005.
17. Lozano, A., F. R. Farrokhi, and R. A. Valenzuela, "Lifting the limits on high-speed wireless data access using antenna arrays," *IEEE Communications Magazine*, Vol. 39, No. 9, 156–162, September 2001.
18. Winters, J. H., "Smart antennas for wireless systems," *IEEE Personal Communications Journal*, Vol. 5, No. 1, 23–27, February 1998.
19. Dessouky, M. I., H. A. Sharshar, and Y. A. Albagory, "Improving

the cellular coverage from a high altitude platform by novel tapered beamforming technique," *Journal of Electromagnetic Waves and Applications*, Vol. 21, No. 13, 1721–1731, 2007.

20. Varlamos, P. K. and C. N. Capsalis, "Electronic beam steering using switched parasitic smart antenna arrays," *Progress In Electromagnetics Research*, PIER 36, 101–119, 2002.
21. Mitilineos, S. A., C. A. Papagianni, G. I. Verikaki, and C. N. Capsalis, "Design of switched beam planar arrays using the method of genetic algorithms," *Progress in Electromagnetics Research*, PIER 46, 105–126, 2004.
22. Laohapensaeng, C. and C. Free, "An adaptive antenna using genetic algorithm," *Microwave Conference Proceedings, 2005, APMC 2005, Asia-Pacific Conference Proceedings*, Vol. 5, 4, 2005.
23. Cengiz, Y. and H. Tokat, "Linear antenna array design with use of genetic, memetic and Tabu search optimization algorithms," *Progress In Electromagnetics Research C*, Vol. 1, 63–72, 2008.
24. Donelli, M., S. Caorsi, F. DeNatale, M. Pastorino, and A. Massa, "Linear antenna synthesis with a hybrid genetic algorithm," *Progress In Electromagnetics Research*, PIER 49, 1–22, 2004.
25. Mitilineos, S. A., S. C. Thomopoulos, and C. Capsalis, "Genetic design of dual-band dipole arrays, with elements failure correction, retaining constant excitation coefficients," *Journal of Electromagnetic Waves and Applications*, Vol. 20, No. 14, 1925–1942, 2006.
26. Varlamos, P. K. and C. N. Capsalis, "Design of a six-sector switched parasitic planar array using the method of genetic algorithms," *Wireless Personal Communications Journal*, Vol. 26, No. 1, 77–88, August 2003.
27. Ponnekanti, S. and S. Sali, "Non-linear interference cancellation techniques for electromagnetically dense propagation environments," *Progress In Electromagnetics Research*, PIER 18, 209–228, 1998.